Hydrol. Earth Syst. Sci. Discuss., 10, 12861–12904, 2013
www.hydrol-earth-syst-sci-discuss.net/10/12861/2013/
doi:10.5194/hessd-10-12861-2013

Hydrology and Earth System Sciences
Discussions
Open Access

Retrospective analysis of a non-forecasted rain-on-snow flood in the Alps – a matter of model-limitations or unpredictable nature?

O. Rössler[1], P. Froidevaux[2], U. Börst[3], R. Rickli[4], O. Martius[2], and R. Weingartner[1]

[1]Oeschger Center for Climate Change Research and Group for Hydrology, Institute of Geography, University of Bern, Switzerland
[2]Oeschger Center for Climate Change Research and Swiss Mobiliar Lab for Climate Impact Research and Natural Hazards, Institute of Geography, University of Bern, Switzerland
[3]Department of Geography, University of Bonn, Germany
[4]BKW FMB Energy AG, Bern, Switzerland

Received: 20 September 2013 – Accepted: 18 October 2013 – Published: 29 October 2013

Correspondence to: O. Rössler (ole.roessler@giub.unibe.ch)

Published by Copernicus Publications on behalf of the European Geosciences Union.

Abstract

On 10 October 2011, a rain-on-snow flood occurred in the Bernese Alps, Switzerland, and caused significant damage. As this flood peak was unpredicted by the flood forecast system, questions were raised concerning what has caused this flood and whether it was predictable at all. In this study, we focused on one valley that was heavily hit by the event, the Loetschen valley (160 km^2), and aimed to reconstruct the anatomy of this rain-on-snow flood from the synoptic conditions represented by European Centre for Medium-Range Weather Forecasts ECWMF analysis data, and the local meteorology within the valley recorded by an extensive met-station network. In addition, we applied the hydrological model WaSiM-ETH to improve our hydrological process understanding about this event and to demonstrate the predictability of this rain-on-snow flood.

We found an atmospheric river bringing moist and warm air to Switzerland that followed an anomalous cold front with sustained snowfall to be central for this rain-on-snow event. Intensive rainfall (average 100 mm day^{-1}) was accompanied by a drastic temperature increase (+8 K) that shifted the zero degree line from 1500 m a.s.l. to 3200 m a.s.l. in 12 h. The northern flank of the valley received significantly more precipitation than the southern flank, leading to an enormous flood in tributaries along the northern flank, while the tributaries along the southern flank remained nearly unchanged. We hypothesized that the reason for this was a cavity circulation combined with a seeder-feeder-cloud system enhancing both local rainfall and snow melt by condensation of the warm, moist air on the snow.

Applying and adjusting the hydrological model, we show that both the latent and the sensible heat fluxes were responsible for the flood and that locally large amounts of precipitation (up to 160 mm rainfall in 12 h) was necessary to produce the estimated flood peak. With considerable adjustments to the model and meteorological input data, we were able to reproduce the flood peak, demonstrating the ability of the model to reproduce the flood. However, driving the optimized model with COSMO-2 forecast data, we still failed to simulate the flood precisely because COSMO-2 forecast data under-

HESSD
10, 12861–12904, 2013

estimated both the local precipitation peak and the temperature increase. Thus, this rain-on-snow flood was predictable, but requires a special model set up and extensive and locally precise meteorological input data, especially in terms of both precipitation and temperature.

1 Introduction

In the early morning on 10 October 2011, the discharge of several mountain rivers in the Bernese Alps and the northern Valais Mountains in Switzerland increased very rapidly. In the Loetschen valley, four small tributaries of the main river Lonza rushed to the valley floor, causing heavy erosion and transporting considerable amounts of debris by saturated transport. In addition, extended overland flow was observed at higher elevations. The floods generated a large debris fan at the foot of the south-facing slope, whereas tributaries at the north-facing slope showed no significant runoff. The only road connecting all villages in the Loetschen valley was buried several hundred meters, and the underlying water reservoir was filled with 200 000 m^3 debris. Fortunately, there were no injuries, but the flood caused total damages of approximately 90 Mio CHF (Andres et al., 2011).

Flood predictions using coupled numerical weather predictions (NWP) and deterministic hydrological models are today a standard approach that is further extended using ensemble forecast systems (EPS) to cope with model uncertainties (see review of Cloke and Pappenberger, 2009). In Switzerland, this approach is implemented by combining COSMO and COSMO-LEPS forecast data with an extended HBV hydrological model (Bundesamt für Umwelt, 2009). A dense network of discharge gauging stations is maintained, and the BAFU operationally forecasts the discharge of several river systems. In fact, rising water levels for the river Kander (Bernese Oberland) were predicted for this flood, but the peak was strongly underestimated – below the warning level.

Shortly after this extreme event, the following questions were raised: (a) what exactly caused the flood? and (b) why was this event not properly forecasted to warn the public? The authority in charge of hydrological warnings, the Federal Bureau for Environment (BAFU), commissioned a study to analyze the causes of this flood event. The present study is based on a contribution to the BAFU study (Rössler et al., 2013).

The flood was preceded by a special weather situation: during the first week of October 2011, a strong high-pressure system brought a period of warm and clear weather to the Swiss Alps. These stable weather conditions were replaced by a cold front system on 6 October that led to extensive snow fall (1–2 m snow depth) down to 1200 m a.s.l. and that lasted until 9 October. After some hours of sunshine on 9 October (hereafter 9 October), a warm and moist northwest front with locally heavy rainfall reached the Alps in the early morning on 10 October (hereafter 10 October). This history indicates that the flood was a typical rain-on-snow event.

Rain-on-snow floods are known as one of five flood – types occurring in temperate climate mountain river systems (Merz and Blöschl, 2003). While most studies about rain-on-snow events have been done in North America, this flood-type is also reported from Europe (e.g. Sui and Koehler, 2001), Japan (Whitaker and Sugiyama, 2005), and New Zealand (Conway, 2004). Characteristically, the rain is partially stored in the snow cover up to the liquid water holding capacity ($\sim$ 10.0 % snow water equivalent (SWE) of the snow water) and is later released from the snow cover. The melting energy from the liquid precipitation causes enhanced direct runoff that is due to both increased snowmelt and due to decreasing water holding capacity; hence, more water is released from the snow. The snow cover can therefore be an amplifying factor for floods, or it can have a curbing effect if the snow cover is too thick or the melting energy too low.

According to McCabe et al. (2007), the main driving factors for a rain-on-snow flooding are the extent of the snow-covered area, the freezing and thawing elevations, the water equivalent of the snow cover, and the liquid precipitation amount. Merz and Blöschl (2003) also stress the importance of latent heat input and point to the occurrence of extended overland flow during rain-on-snow-events because soils are saturated by antecedent snowmelt processes.

In general, the prediction of floods remain challenging as small differences in precipitation and temperature cause strong biases in the hydrological prediction, especially in mountainous areas with small response times and the importance of determining the snow limit (Jasper et al., 2002). The prediction of rain-on-snow events is even more challenging as it requires accurate information on snow covered area and snow water equivalent. McCabe et al. (2007) stated that the prediction of rain-on-snow events is not only limited by the meteorological input parameter, but also due to insufficient knowledge about the important processes involved. The latter is even more valid for Europe with far less research attention on rain-no-snow events than for instance in North America. Hence, data of observed rain-on-snow events and case studies revealing in detail the causes and process-sequences of this important and fascinating hydro-meteorological process is required to improve our process understanding and to improve the forecastability of such extreme events.

Due to the hydro-meteorological character to this rain-on-snow-flood in the Loetschen valley, we chose a comprehensive approach by aiming to reconstruct the flood anatomy starting from the synoptic-scale conditions down to the local observations. First, to broaden our current process-understanding of rain-on-snow floods, we want to elucidate the relevant synoptically and locally observed processes behind this event and to compare them with the key processes of typical rain-on-snow events. Second, to estimate the predictability of the rain-on-snow flood, we applied a hydrological model (WaSiM-ETH) to evaluate its ability to reproduce the local flooding. Third, we assessed the predictability of the rain-on-snow flood by driving the hydrological with COSMO-2 forecast data. This will lead to a final assessment of past and future predictability of this rain-on-snow event.

2 Materials and methods

2.1 Study area

The Loetschen valley lies just south of the Bernese Alps, which acts as the first barrier for the predominantly northwestern atmospheric inflows. As a result, the highest annual precipitation amounts in Switzerland are found within this mountain range (Jungfrau, Eiger, Mönch, > 3600 mm per year, Kirchhofer and Sevruk, 2010). The Loetschen valley is situated in the transition zone between this area of highest precipitation amounts and the driest region in Switzerland (Rhone valley, Stalden, 535 mm per year). The Loetschen valley (Fig. 1) stretches from 600 m at the southern outlet up to approximately 4000 m a.s.l., with a mean elevation of 1800 m a.s.l. The valley bottom extends from the southwest to the northeast and rises slightly from approximately 1200 m a.s.l. to 2100 m a.s.l. at the glacier tongue; all of the surrounding mountain ridges are approximately 3000 m a.s.l., and the mountain tops are higher. Dominant vegetation types are coniferous mountain forests and alpine pastures. Nearly 18 % of the catchment is glaciated. The Lonza is the main river in the valley and is fed by numerous small tributary rivers from the north- and south-facing slopes and the highest elevations. The black arrows in Fig. 1 mark the rivers that had extraordinary floods during the October event (from left to right: Ferdenbach, Milibach, Tännbach, and Gisentella). Notably, none of the rivers on the north-facing slope showed any extreme flooding.

2.2 Methods for reconstructing the flood

2.2.1 Reanalysis and soundings data

The four day synoptic evolution preceding the event is analyzed using the Era-Interim-reanalysis dataset from the European Center for Medium-Range Weather Forecasts (ECMWF) (Dee et al., 2011). This reanalysis dataset results from a general circulation model that is continuously forced by a complex assimilation of various observations of the atmosphere, ocean, and land surface. It is commonly used for the retrospective analysis of meteorological situations. The main atmospheric variables are available on a three dimensional grid (1° horizontal resolution, 90 vertical layers) every six hours. In addition to these gridded data, vertical characteristics of the atmosphere recorded from weather balloons launched in Payerne (cp. Fig. 1) were analyzed. The Payerne upper air soundings station is located in the Swiss Plateau 80 km northwest of the Loetschen valley (upstream of the October flood event, see Fig. 1). These weather balloons are launched twice a day and provide high resolution profiles of temperature, humidity, wind velocity, wind direction and pressure. Here, we compared radio-sounding data from the day before (9 October, 0:00 UTC) with data from the day of the flood event (10 October, 0:00 a.m. UTC).

2.2.2 Local meteorological observations

The local development of the hydro-meteorological event is analyzed in detail using data from a dense network of observations in the Loetschen valley. The Lonza river discharge is officially measured by the BAFU at the center of the valley (Blatten gauge, Fig. 1), and inflow to the reservoir of the EnAlpin hydropower was provided by the operating company during the extreme event in October 2011 (Ferden reservoir gauge, Fig. 1). Eight meteorological stations are distributed in the valley. These stations are located on both sides of the valley at different elevations. Two stations are operated by the Institute for Snow and Avalanche Research (SLF), and one is operated by a private weather service, MeteoMedia. All other stations were set up by the Department of Geography, University of Bonn (GIUB) during a previous research project (Börst, 2005, cp. Table 1). This high network density enables a very detailed analysis of the meteorological conditions in the valley during the rain-on-snow-event. The meteorological stations are equipped with standard measuring devices for temperature, precipitation, air humidity, wind speed, wind direction, global radiation, and snow depth. Table 1 summarizes the location and equipment at each station; IDs refer to the numbers in Fig. 1.

HESSD
10, 12861–12904, 2013

All rain gauges are unheated; therefore, precipitation depth and duration during snow fall and in the transition from snow to rainfall must be analyzed with caution.

2.2.3 Hydrological modeling

The retrospective modeling of the flood was conducted using the WaSiM-ETH distributed hydrological model. This physically based, fully distributed model has been successfully applied to several alpine catchments and research questions (Verbunt et al., 2003; Rössler et al., 2012). Rössler and Löffler (2010) demonstrated the ability of this model to reproduce the water balance and runoff in the Loetschen valley. Basically, WaSiM-ETH solves the water balance equation for each raster cell using physically based equations; for example, infiltration is calculated using the Green and Ampt (1911) approach, and water fluxes within the unsaturated zone are based on the Richards equation. Lateral fluxes are less adequately reproduced; interflow is generated at each raster cell; however, the interflow is not routed to the underlying raster cell, but rather, it is directly assigned to the nearest drainage channel with a topography-derived travel-time delay. WaSiM-ETH requires spatial data of soil and land use types and a digital elevation model. The characteristics of the two former data sets must be parameterized according to the assigned types (e.g., soil hydraulic properties, soil magnitude, root depth, and leaf area index). Meteorological information for each raster cell is generated by interpolating meteorological point data to the entire catchment, which can be achieved in several ways. The simplest methods are the Thiessen polygon (TP) interpolation and the inverse distance weighting (IDW) methods; these methods depend solely on the spatial distribution of the meteorological stations. A more advanced method is the combination of IDW with an elevation-dependent regression (IDWREG). Elevation-dependent regression can be useful in areas with high elevation gradients, such as the Loetschen valley. In addition, WaSiM-ETH is able to make use of externally processed data, such as the COSMO forecast data sets. All of these methods are described in more detail by Schulla (2012). As the focus of this study is the simulation of a rain-on-snow-event, the reproduction of snowmelt is crucial. In

WaSiM-ETH, different methods can be applied. The standard technique is a degree-day-factor-model (hereafter called SM1) that can be extended to a degree-day-factor model that includes wind speed. Finally, WaSiM-ETH offers the possibility to consider latent heat fluxes as they occur during rain-on-snow events using an energy balance model after Anderson (1973) (hereafter called SM2). For precipitation depths of more than 2 mm day^{-1}, the SM2 approach calculates the snowmelt as a function of sensible heat (degree-day-factor with wind speed), latent heat (degree-day-factor with saturation deficit), radiation melt (1.2$\cdot$ air-temperature), and energy from liquid precipitation (0.0125$\cdot$ precipitation $\cdot$ air-temperature) (cp. Schulla, 2012). When the precipitation amount during one time step is less than 2 mm, melt is calculated using the simple degree-day-factor model (SM1). In addition, the SM2 also subdivides the snow cover into a liquid and a solid part and the maximum water holding capacity has to be parameterized (standard 10 %, Schulla, 2012).

To analyze the key processes causing the flooding, we applied a previously calibrated version of WaSiM-ETH, version 7.9.11 (Rössler and Löffler, 2010). The model has a temporal resolution of one hour and a spatial resolution of 50 m $\times$ 50 m. The model was calibrated against discharge for the year 2002 and validated for 2003–2007. Statistical measures such as the Nash–Sutcliffe-Index (cal.: 0.84, val.: 0.8), Pearsons-R (cal.: 0.94, val.: 0.95) and the Index of Agreement (cal.: 0.96, val.: 0.95), in addition to the water balance, demonstrated the model's ability to reproduce discharge from the Lonza catchment (Rössler and Löffler, 2010).

2.2.4 Stepwise adjustments of the standard hydrological model

The hydrological modeling should not be understood as an end in itself but as a tool to improve the process understanding and the forecast. The former is especially the case if models are not consistent with the observations (Beven, 2001). Hence, in this study, we wanted to determine which parameters, algorithms and data sets must be adjusted to simulate this rain-on-snow-flood. We used the previously calibrated model as a starting point, and we gradually changed the model to represent the flood peak in the Lonza River during this event. Each gradual change is underpinned by hypothetical assumptions of the underlying processes to reach a better understanding of the processes involved. Changes are made to input data sets, single model algorithms, parameter values, and the temporal resolution.

1. Model parameter adjustments
   In the course of this study, three model parameters ("fraction of direct flow from snowmelt", "runtime of direct flow and interflow", and the melt-factors of the snow-modules) were adjusted to account for deviations between the modeled and the observed discharge. Melt factors determine the amount of water that is melted per time step and the energy available (latent and sensible). The melt factors were adjusted with respect to both discharge and snow depth. The modeled snow depth is calculated from the SWE amount, assuming a snow density of $0.1\,\mathrm{g\,cm^{-3}}$. The "fraction of snowmelt that is direct runoff" defines the proportion of liquid water in the snow cover that infiltrates into the soils and the proportion that is directly assigned to surface runoff. In this study, we increased this value considerably (from 10 % to 90 %) under the assumption that the soil below the snow cover was saturated very quickly and directly cause surface runoff. For the same reasons, we decreased the "response times of direct flow and interflow" that indicate the response time to precipitation events in the catchment. These parameters are typically derived from a hydrograph if observations are available.

2. Changing the snow module in WaSiM-ETH
   We used two of the four different snow modules available in WaSiM-ETH. First, we applied the simple but straightforward degree-day-approach (SM1). Second, a snowmelt model was used that considers not only the sensible heat (temperature) as the degree-day-module does but also the latent energy (SM2). The performance of these modules indicates whether sensible heat alone or a combination of latent and sensible heat controls snowmelt and runoff generation.

3. Input data sets
Precipitation is a crucial input data set; accordingly, the applied regionalization approach and the chosen meteorological stations determine the modeling results. Initially, we used the IDWREG approach based on the same official meteorological stations as used in the first calibration and added one additional stations (Gandegg, Fig. 1) situated directly at the center of action. Subsequently, we used a refined data set that incorporates all official (see Fig. 1) and all private meteorological stations available (see Table 1), despite their inaccuracies in recording solid vs. liquid precipitation. Because of the snow fall measurement were best on official meteorological stations only as all private stations are unheated, we fitted the precipitation against snow depths (assuming a density of 0.1 $g\,cm^{-3}$) measured at the SLF IMIS station Gandegg. This resulted in a correction factor of 0.85 for snow fall. In terms of liquid precipitation an overestimation is likely as this measured rainfall is biased by the snow in the rain gauge. Here, we also applied a reduction of 15 % (up to 24 mm). As this procedure is quite uncertain, we evaluated these corrections against discharge and found the best performance using this correction.

2.2.5 Test of the event predictability

To test the predictability of the event, we applied the optimized model that best reproduced the flood peak and used the COSMO-2 forecast model data (Meteoschweiz, 2011) as meteorological input data. COSMO-2 is a high-resolution numerical weather forecast model with a spatial resolution of 2.2 km × 2.2 km. It is used by several meteorological services in Europe; in Switzerland, it is applied in combination with the coarser resolution COSMO-7 model. COSMO-2 is updated eight times a day and provides a forecast of 24 h. Here, we used COSMO-2 temperature and precipitation data from 18 h, 12 h, and 6 h in advance of the flood peak on Monday, 10 October 2011, 12:00 UTC.

HESSD
10, 12861–12904, 2013

3 Results

3.1 Reconstructing the weather conditions

The weather conditions in the Loetschen valley between 7 October and 10 October were characterized first by a drastic change from warm, dry, and bright weather conditions to cold temperatures and snowfall on 7 October (−14 K from 6 October, 11:00 UTC to 7 October, 11:00 UTC), and second by a rapid change back to warm conditions with significant amounts of liquid precipitation on 10 October (+8 K). The large-scale atmospheric flow evolution responsible for these drastic and rapid changes in temperature and precipitation were as follows:

A very active cold front associated with a low pressure system over Scandinavia led to a distinct temperature contrast across the Swiss Alps on Friday 07 October 2011 (Fig. 2a). After the frontal passage a breezy northwesterly of polar air brought prolonged snowfall on Saturday 08 October (Fig. 2b). The temperature at 850 hPa was close to zero, and the snowfall limit was located at approximately 1500 m a.s.l. On Sunday 09 October (Fig. 2c), the northwesterly flow weakened, and around midnight, an active warm front associated with a low pressure system over Iceland reached Switzerland from the northwest. This warm front was of crucial importance for the flooding for two reasons. First, the warm front was accompanied by a rapid and dramatic rise of the temperature. Second, it was followed by a very strong northwesterly flow bringing warm and remarkably moist air into the Alps (Fig. 2i).

This warm front was part of a narrow band of moist tropical air ranging from the subtropical Atlantic around the Azores High to the Alps (Fig. 2f). It owned the characteristics of an atmospheric rover (AR). The vertically integrated precipitable water exceeded 20 mm, wind speed in the lowest two kilometers was greater than 12.5 $\mathrm{m\,s^{-1}}$, it was a few hundred kilometers wide and it extended for thousands of kilometers across the North Atlantic (e.g., see Ralph et al., 2011, Fig. 2d–f).

The passage of the cold and the warm fronts at the surface was associated with the passage of a high potential vorticity (PV) trough, or positive PV anomaly, at tropopause

HESSD
10, 12861–12904, 2013

levels of the atmosphere (red line in Fig. 2d–f). Such upper level PV anomalies influence the structure of the atmosphere underneath them such that colder air and reduced stability are typically found below (e.g., Schlemmer et al., 2010). The red line in Fig. 2d–f show the subsequent development of the PV anomaly. We observe that the excursion of polar air towards the equator is located below the positive PV anomaly and that the passing of the cold and warm fronts correspond to the upstream and downstream flanks of the trough, respectively. Additionally, the boundary of the area with less than two PV units corresponds remarkably well to the AR impinging on Switzerland on 09 October. A more general statement is that the passage of a trough followed by the passage of a ridge and the associated major variations of upper level PV must coincide with important changes in stability, vorticity and temperature in the mid to low troposphere. Such rapid and intense changes of the flow properties over areas as large as the alpine range can only coincide with the meridional transport of air masses and abrupt air mass transitions.

The vertical extent of the change from cold and dry to warm and wet atmospheric conditions was captured by the upper air sondes launched in Payern at 00:00 UTC on 09 October and 10 October (Fig. 3). The comparison of both profiles shows that the freezing level rose from 1500 to 3000 m a.s.l. in 24 h. This strong warming was associated with an equally drastic moistening as depicted by the rise of the zero-degree dew point temperature from approximately 1500 to 3000 m a.s.l. In the profile from 10 October, two different air masses can be distinguished. A very stable (isothermy) and cold layer extended from the surface up to 800 hPa and is overlaid by a less stable layer. This points to the blocking along the northern face of the Alps at the time of the warm front arrival. This cold pool might have played a role in determining the distribution of precipitation by pre-lifting the air and creating a level of wind shear (between the retarded blocked flow and the fast unblocked flow). Strong shear can favor the development of turbulent cells embedded in a cloud layer and associated up- and downdrafts, which in turn might influence precipitation growth mechanisms significantly (see, for example,

HESSD
10, 12861–12904, 2013

Houze and Medina, 2005). The wind direction (not shown) was mostly NW to N from 2000 m upwards.

That the air was lifted over the Alps rather than being blocked by the Alpine barrier can be determined from the Froude number (F) (Reinecke and Durran, 2008). F is the ratio between the kinetic energy of the wind and the energy required to pass over a barrier. If F is larger than 1, the air can surpass the Alpine barrier. F was > 1 from 2200 m upwards (not shown), indicating that the air masses located approximately 2200 m a.s.l. above Payerne were flowing over the Alps, resulting in a North Foehn condition. Values of $F < 1$ below 2200 m a.s.l. confirm the presence of a blocked cold air pool near the surface.

It is interesting to compare the temperature profiles retrieved from the upper air sounding with the 2 m temperature profiles of the Loetschen valley retrieved from surface thermometers (Fig. 4). While the vertical profiles are very similar on 09 October at 00:00 UTC, the valley floor is significantly cooler than the free air on 10 October at 00:00 UTC. This difference might be the result of intense snow melt during the passage of the warm front. Snow melt requires significant energy input from the surface air and evidence for it is given later by station measurements. The soundings themselves also show that large scale conditions were very suitable for widespread and intense snow melt. Remarkable is that not only the temperature but also the dew point temperature reached positive values up to 3000 m a.s.l. A positive dew point temperature indicates that the ambient air contained more moisture than the air in equilibrium with the snow (the surface air in direct contact with the snow pack has a temperature and a dew point temperature of 0 °C during a melt event). Ambient air coming into contact with the snow pack is cooled, i.e. sensible heat flux into the snow pack takes place, and when the air temperature reaches the dew point condensation sets in. Each gram of condensed water vapor releases sufficient energy to melt 7 g of snow; therefore, snow melt is significantly enhanced by latent heat transfer in the case of positive dew point temperature.

HESSD
10, 12861–12904, 2013

In summary, the following large-scale atmospheric ingredients predetermined the flood in Loetschental: the North Foehn flow on 08 October was remarkably strong due to a large pressure gradient over the Alps (between the Azores high and the Scandinavian low). The advected polar air was anomalously cold resulting in a snow limit that was anomalously low for the season so that an significant amount of fresh snow was accumulated down to a relatively low altitude. This situation would have been harmless, however, without the sudden arrival of warm and moist northwesterly air (AR) on the evening of 09 October and significant amounts of rainfall on 10 October.

3.2 Local meteorological conditions

Eight stations distributed throughout the Loetschen valley confirmed the course of the general weather conditions previously described. Figure 5a–d summarizes the development of the 2 m-air temperature (Fig. 5a), the relatively humidity (Fig. 5b), the accumulated liquid (Fig. 5c) and the solid precipitation (Fig. 5d) from 7 October to 10 October at each station. The temperature observations show a strong cooling below freezing point above approximately 1470 m a.s.l. (Ried), confirming the previous assumption about snow limit. Only the Wiler station, at 1415 m, experienced slightly positive temperatures. On 09 October, the stations at the valley bottom recorded an increase of temperature up to 8 K temperature increases, which might indicate an intermediate period of clear sky; in contrast, no significant diurnal temperature cycle was recorded at higher elevations. Between 09 October in the evening and the morning of 10 October, a rapid warming was recorded at all stations (+8 K). This warming coincided with the arrival of the warm front and was most pronounced close to the Northern crest, as indicated by the Sackhorn and Gandegg stations (cp. Fig. 1).

The temporal evolution of liquid (Fig. 5c) and solid (Fig. 5d) precipitation was similar at all stations, but the recorded precipitation amounts varied significantly. Rainfall was generally higher at the higher altitudes and, more interestingly, significantly more rain fell on the south-facing slope than on the north-facing slope. For example, the Chumme station recorded more than twice as much precipitation (108 mm) than the

Mannlich station (42 mm) at the same elevation on the opposite slope. The highest precipitation amounts at the valley bottom were found near Wiler; precipitation first decreased going eastward (Ried) before increasing with increasing elevation (comparing Wiler – Ried – Grund – GrossiTola). Snow depth was more linearly correlated to altitude than rainfall was, with snowfall starting earlier, lasting longer and more intensively at higher elevations. For example, the snow amounts recorded at Chumme and Mannlich are similar. Evidence for snow melt is given by the rapid decrease of snow depths, amounting to decreases of 40 cm at Chumme and Mannlich and 60 cm at Gandegg in six hours. The onset of snow melt is delayed by several hours going from 1900 m (Grund) to 2200 m (Chumme and Mannlich) to 2700 m (Gandegg) because of lower temperatures at higher elevations.

The measured wind provides evidence for the leeward-side air circulation during the event. Figure 5 shows diagrams of the recorded wind directions on 10 October. Sackhorn station is the only one recording a NW wind consistent with the synoptic scale flow. It is the only station directly exposed to the incoming north westerlies. All of the other stations, located on the lee of the northern crest, registered local circulations inside the valley. Ried, Grund and Grossi Tola stations along the WSW–ENE valley axis recorded along valley winds with a predominance of wind in the downslope direction. At Wiler, the wind direction was highly variable. Both mid-slope stations, Chumme and Mannlich, show wind directions similar to those at the valley bottom. Particularly interesting is the Gandegg station, which is the only one recording a SE wind. Remarkably, the wind direction at Gandegg was opposite of the wind direction at Sackhorn, which is in linear distance only 1250 m apart.

While the macroscale analysis showed that the synoptic situation was conductive to a rain-on-snow event with the passage of a very active cold front and a very active warm front, the dense network of meteorological stations points to variations at the local scale. The rain-on-snow event was intense close to the northern crest (10 K temperature increase in 12 h, 160 mm of rain in 6 h and a snow depth decrease of 60 cm in 12 h at Gandegg) and gradually less intense from north to south across the valley.

HESSD
10, 12861–12904, 2013

Rainfall totals decreased by a factor of 4 along a 6 km cross section between Gandegg and Mannlich. This remarkably steep rainfall gradient indicates kilometer-scale heterogeneity of the atmospheric flow.

The interaction of the synoptic scale atmospheric flow with the complex alpine topography can trigger local extreme weather via many different processes. We postulate that the development of a so-called cavity circulation in the lee of the northern crest (see Fig. 6) might have led to the observed rainfall gradient. Cavity circulations are rather frequent in the Northern Alps and often captured by webcams. Typically, they are recognized through the formation of so-called banner clouds (see for example Wirth et al., 2012). We have no proof of a cavity circulation early on 10 October, but some evidence points towards its probable occurrence. First, the wind station at Gandegg recorded upslope winds opposite to the background wind direction. Second, relative humidity and webcams indicated the occurrence of a surface cloud along the upper southward facing slope. Third, the Froude number was much larger than unity, indicating the presence of a "flow over" condition necessary for the formation of gravity circulation. The cavity circulation would have led to an upslope ascent associated with adiabatic cooling and low level saturation which enhanced snow melt very efficiently through heat and moisture supply. Rainfall can also be enhanced significantly by low level clouds through the seeder-feeder effect. Indeed, in the case of low level clouds, the hydrometeors created higher above by the seeder cloud fall through a saturated layer and are not vaporized. They collide with the low level droplets so that rainfall efficiency has the potential to rise significantly. Forced ascent from the topography and saturated air is likely to have produced a low level cloud on the windward side of the northern crest as well; therefore, intense snow melt and intense precipitation is likely to have occurred on both sides of the Loetschen valley's northern crest. We do not have measurements from the windward side, but flooding has been reported from the affected Gasteren valley, which contributed to the 100 yr flood event in the Kander valley.

The rapid decrease of snow depth as measured at the Gandegg station might be interpreted as either efficient snow melt accelerated by high surface water vapor and/or

HESSD
10, 12861–12904, 2013

snowpack melt and compaction by locally enhanced rainfall. The rain was most likely stored in the fresh snowpack until saturation was reached. Additionally, the snowpack most likely acted as a runoff enhancer by trapping a portion of the rain before releasing the liquid water.

3.3 Retrospective modeling of the event

To gain more knowledge about the involved processes and flood predictability, we retrospectively modeled the event, based on a previously calibrated version of the model. First, we simulated the flood discharge at two gauges, Lonza-Blatten (BAFU) and Lonza-Ferden (EnAlpin), to validate the performance of both the initial model and the adjusted model. In a second step, modeled discharge was evaluated for the ungauged tributary river of the Lonza at the southern slope, Milibach, affected by the highest precipitation amounts and flooding (estimated 32 $m^3 s^{-1}$, unpublished data, Geoplan Naturgefahren).

Figure 7 comprehensively illustrates the modeled temperature, precipitation and the resulting simulated and observed discharge for Lonza at Blatten and Ferden during the period of interest for standard and refined meteorology. At first, we focus on the standard meteorology: The temperature shows diurnal variations clear 01 October to 06 October. Then, along with a drastic temperature decrease, snow began to fall and continues to fall constantly for two and a half days. Intense rainfall accompanied by temperatures rising to slightly positive values (+8 K) starts after a short period of dry conditions. The observed runoff corresponds to these weather conditions, with diurnal runoff cycles of glacier melt followed by constant base flow during the cold period and an abrupt rise in flow around noon on 10 October. Using the previously calibrated, mean-flow focused hydrological model (Fig. 7, left, blue line), the general sequence of the runoff is reproduced, but the flood-peak on 10 October is strongly underestimated, especially for the Lonza at Ferden (Lonza, Blatten: 42 $m^3 s^{-1}$ modeled, 64 $m^3 s^{-1}$ observed; Lonza, Ferden: 60 $m^3 s^{-1}$ modeled, 120 $m^3 s^{-1}$ observed).

HESSD
10, 12861–12904, 2013

Therefore, two different peak-optimized model versions were set up to reproduce the flood maximum for Lonza at Blatten and Lonza at Ferden with increasing degrees of deviation from the standard model. One model version was obtained by adjusting only one model parameter (green line, Fig. 7, left) under standard meteorology; the fraction of snowmelt that is directly routed to the drainage without infiltration was increased from 10 % to 90 %. In the second model version (orange line, Fig. 7), we used SM2, which extends the sensible heat determined by the degree-day approach by incorporating the latent heat transfer from precipitation, radiation, wind, and humidity. Both model versions show a much better representation of the flood peak and are able to reproduce the flood for the Lonza at Blatten, while underestimating the flood at the underlying gauge for the Lonza, Ferden.

The third model version used refined meteorology from our meteorological station network for the model inputs and adjusted parameters for the snow (SM2 approach) and routing modules (magenta line, Fig. 7, right); the model parameters were adjusted to simulate the Milibach catchment flood peak (see below). This model version is able to reproduce both flood peaks, but overestimated runoff in the days before the event. This "best" model was developed by refining the meteorological condition in the catchment:

Local observations indicated a strong heterogeneous distribution of liquid precipitation with a focus on the northern rim of the valley (see the section on local meteorology). We compared these observations with the modeled precipitation distribution and found that the standard model regionalization – based on official meteorological stations and the Gandegg station – had a homogenous, strongly height-dependent precipitation pattern (Fig. 8, upper panel, standard meteorology) with miner valley intern variations. Accordingly, the precipitation sums on the north-facing slope are overestimated (110 mm modeled vs. 42 mm measure at Mannlich, cp. Fig. 4d) and those on the south-facing slope are underestimated. We refined the interpolation by including all of the meteorological stations, and we specified a mainly southwest-northeast precipitation field to correspond with the topography of the valley (Fig. 8, lower panel, refined meteorology). The resulting liquid precipitation distribution is closer to that described in the local meteorology section.

The effect of this refined meteorology is analyzed using the model performance in the Milibach tributary catchment. Figure 9 shows the modeled and observed runoff as well as weather and snow depth at the Gandegg meteorological station, which is located within the Milibach catchment. The left panel summarizes the performance for the standard meteorology with both snow melt algorithms (SM1 and SM2) applied, while the right panel shows the model output for the SM2 melting using the refined meteorology. For the latter, we also adjusted the snow melt parameters to reproduce the snow cover depletion correctly. Under standard meteorology and standard parameter setting, the SM1 approach is not able to melt the snow cover, because energy input from sensible heat (temperature) was too low at this elevation. Using the SM2 approach, snow is melted, but both snow accumulation and snow melt were overestimated. These limitations were removed in the adjusted model version under refined meteorology. In addition, we increased the water holding capacity from 10 % to 20 % of SWE to account for overestimations of discharge at gauges in Blatten and Ferden. Under both SM2 approaches and both water holding capacities, the snow is saturated after the first rainfalls shortly after midnight on 10 October.

Two conclusions can be drawn from this comparison: (1) the usage of the extended snow melt module SM2 (light blue line) is necessary to reproduce the snow melt, and (2) using the adjusted meteorology and model (right panel) provides a better representation of the snow cover depth and a higher amount of rainfall within the Milibach catchment. However, none of the models are able to reproduce the observed discharge peak (maximum flow is $9.3\,m^3\,s^{-1}$ simulated vs. $32\,m^3\,s^{-1}$ estimated). Only a drastic reduction of the running times for direct-flow and interflow from this subcatchment (routing parameters) leads to a further concentration of discharge and a peak of $24.6\,m^3\,s^{-1}$ (Fig. 9, dotted orange line). These two parameters are normally calibrated against an observed hydrograph, but as the Milibach catchment is ungauged, the adjustment of the parameters is speculative but still within a reasonable range.

HESSD
10, 12861–12904, 2013

Applying this adjusted model to the entire Lonza catchment provides the good representation of the flood peak at Blatten and Ferden (magenta line, Fig. 7, right) already described above. However, there are large overestimates in the diurnal melting cycles before the event due to the overestimation of the melting rates. The adjusted model therefore is only valid for the rain-on-snow flood. Still, the reliability of this version of the model for the time of the flood peak is better than the previous versions, as the catchment's internal characteristics, such as precipitation distribution and snow depletion, are incorporated.

The retrospective modeling of the flood event demonstrated the importance of both latent and sensible energy in the melting process, as suggested from the analysis of the local meteorology. Moreover, the refinement of the meteorology was important for representing the strong heterogeneous runoff pattern. Still, some limitations remain in the representation of the flood peak of Milibach (25 $m^3 s^{-1}$ simulated vs. 32 $m^3 s^{-1}$ estimated); these limitations can be ascribed to limitations in the representation of meteorological values, uncertain model parameters and/or uncertainties in the observations. A further increase of local precipitation amounts (+15 %) in the Milibach catchment led to a flood peak of 31 $m^3 s^{-1}$ (not shown here), but resulted in an overestimation at the gauge Lonza, Ferden, too.

Table 2 summarizes the water fluxes and the hydrological runoff coefficients for this event as simulated using the SM2 model under standard meteorology and parameters and under refined meteorology with adjusted parameters. For the two larger catchments, differences between the versions are small, with little less snow and runoff applying the refined meteorology. However, for the Milibach catchment, the changes are significant. The refined meteorology shifts the proportions of solid and liquid precipitation, reducing the influence of snow melt and enhancing direct runoff from rainfall. Because not all snow was melted and soils were filled up during the flood event, there was the potential for an even higher flood. Considering only rainfall as the input, the runoff coefficient Ψ was calculated with $\Psi > 1$, which emphasized the strong contributing role of snow for this event. Assuming snow melt and rainfall contributed equally

HESSD
10, 12861–12904, 2013

to the flood peak, 30 % of the flood water originated from snow in each of the (sub-) catchments. Snow melt contribution under standard meteorology and SM2 approach is remarkably high (at least 62 %).

To conclude, under standard meteorology, the hydrological model is able to approximately reproduce the flood peak at the catchment scale. But a detailed analysis at the subcatchment showed that these reproductions were due to the wrong reasons. Only after the refinement of the meteorology and a more extensive adjustment of model parameter, the hydrological model reproduces flood peak at the catchment and sub-catchment scale reasonable well, and allow for observed processes.

3.4 Predictability of the event

To evaluate the predictability of the event, we used the COSMO-2 forecast data 6, 12, and 18 h in advance of the flood peak as the input data for the selected optimized model. Figure 10 displays rain and snow in the Loetschen valley and discharge at Lonza, Blatten and at Blatten, Ferden. The meteorology was taken from the COSMO-2 output 12 h before the flood peak occurred at 12:00 UTC on 10 October (rain: lightblue bars, snow: white bars; temperature curve in red) and compared with the refined meteorology (rain: blue bars, snow: yellow bars, temperature curve in black). COSMO-2 data (12 h before flood peak) underestimate both the temperature increase and the precipitation amount in the morning of 10 October, resulting in a strong underestimation of the flood peak (25 $m^3 s^{-1}$, 18 h in advance; 24.8 $m^3 s^{-1}$ 12 h in advance; and 35 $m^3 s^{-1}$, 6 h in advance at Lonza, Blatten). The forecast 6 h in advance resulted at least in a flood peak at the 2 yr-return level (35 $m^3 s^{-1}$). This corresponds to a medium hazard level at Lonza, Blatten. Comparing the total precipitation sums on 10 October of the COSMO-2 (Lonza at Ferden catchment: 78 mm, Milibach catchment: 83 mm), standard meteorology (Lonza at Ferden catchment: 69 mm, Milibach catchment: 90 mm), and refined meteorology (Lonza at Ferden catchment: 122 mm, Milibach catchment: 172 mm), and regarding that under the standard meteorology, a higher flood peak was achieved (Fig. 7, left panel), the underestimation of precipitation is not the only crucial deviation. Lower temperature increase in the night and morning of 10 October led to a higher proportion of snowfall instead of rainfall on 10 October and reduced snow melt.

4 Discussion

Extreme flood events are mostly a result of a combination of adverse meteorological events. These events can be adverse either spatially or temporally. While the former relates to the meteorological impact on vulnerable regions (sealed, saturated, steep), the latter relates to the temporal sequence of weather conditions that results in an extreme flood. In the present case, a merely temporally adverse sequence of weather conditions can be traced back to the passage of unusual cold moist air masses followed by warm, moist air masses. The intrusion of the cold air masses in autumn is a normal occurrence. Based on the ECMWF analysis data, we showed that the warm and moist air masses followed a narrow pathway from the subtropes to the extratropics. Such structures are called atmospheric river (AR) (Bao et al., 2006). While ARs are known to cause river flooding, especially on the west coast of northern America (Ralph et al., 2006), little focus has been placed on the effects of ARs in Europe. Knippertz and Wernli (2010) and Stohl et al. (2008) showed the presence of ARs in Europe, but linking these wet air masses to floods has seldom been performed in Europe. Recently, Lavers and others proved that major flood events in Great Britain (Lavers et al., 2011) and annual maxima of precipitation in Europe (Lavers and Villarini, 2013) are directly linked to AR. Stohl et al. (2008) were able to relate two flood events to ARs that were formed by extratropical transitions. Knippertz and Wernli (2010) demonstrated that 90 % of all extratropical transitions cause an AR, but because there are far more ARs than extratropical transitions, not every AR originates in an extratropical transition. In the present study, the AR originated from an extratropical transition (from hurricane Orphelia).

HESSD
10, 12861–12904, 2013

In contrast to the cited studies, this flood event is not only a result of the high precipitation amounts brought by an atmospheric river but also from the accompanied temperature increase. Moreover, ARs often start to rain out when making landfall and mostly trigger high precipitation close to the coast, but in this case, the AR transported large amounts of moisture to the Alpine range, where complex interactions with orography triggered very intense precipitation. The important role of the freezing level and snow-covered area during rain-on-snow events was stressed by McCabe et al. (2007). Minimum and maximum temperature levels must therefore suit the elevation distribution of the affected snow-covered valley to become problematic. Here, the drastic temperature increase during the night of 9 October to 10 October activated the melting of the snow cover up to an elevation of 3000 m a.s.l., which is 81 % (1400 m a.s.l. to 3000 m a.s.l.) of the area. The Loetschen valley was hence a good match to the temperature amplitude; accordingly, 30 % of the total runoff water originates from snowmelt (Table 2).

In addition to this macro scale meteorological situation, we here postulate that this situation was locally exacerbated by a cavity circulation in association with a seeder-feeder cloud system and enhanced rainfall. This interpretation is consistent with findings of several other studies where seeder-feeder effects are known to cause significant local enhancements of the precipitations amounts (e.g., Roberts et al., 2009; Gray and Seed, 2000). In Pennsylvania, Barros and Kuligowski (1998) found that leeward-side effects enhance the local precipitation during rain-on-snow events and that there is a correlation between leeward-side effects and strong hydrological flooding.

The cavity circulation not only enhanced the rainfall amount but also brought warm and moist air masses down to the snow-cover, resulting in intensified latent heat-dominated snowmelt due to condensation, potentially of moisture from the ambient air. High winds, warm and moist air masses and high dew points are repeatedly reported as key factors during rain-on-snow events as they enhance the snowmelt rates drastically, especially for catastrophic rain-on-snow floods such as the floods in 1996 in the Pacific Northwest (Marks et al., 1998) and in northern Pennsylvania (Leathers

HESSD
10, 12861–12904, 2013

et al., 1998). Because our findings are consistent with these studies, we are confident that our conclusions concerning the course of the meteorological processes at the mesoscale are plausible, although we were not able to directly prove that processes we described actually occurred.

The application and the adjustment of the hydrological model for this flood reconstruction confirmed the observed rapid response of the catchment to the rainfall and snow melt. We emphasize the importance of latent energy for the rapid snow melt process because only the snow module considering sensible *and* latent heat flow (SM2) was able to reproduce the snow depletion. The importance of latent and sensible heat for snow melt during rain-on-snow events is consistent with results from other studies, e.g. Marks et al. (1998), in which an energy-balance model was applied to a rain-on-snow event.

Besides the strong energy input, snow cover structure is crucial in explaining the rapid runoff. Kroczynski (2004) compared two similar rain-on-snow events with difference consequences, one leading to a major flood and one without any flooding. He argued that the cause for the major flood was the prior condition of the snow cover (a ripened snow cover) that led to a saturated snow cover. In the present case, the snow cover was not ripe but rather fresh. But, the snow cover up to 2700 m a.s.l. was modeled to be saturated shortly after midnight on 10 October by the lighter preceding rainfall, so the subsequent heavy rainfall (on the morning of 10 October) fell on a saturated snow cover. This is although the water holding capacity was increased from 10 % to 20 % – according to Jones et al. (1983) a reasonable value during intense snow melt periods. The WSL/SLF (in print, 2013) analyzed in a 1-D SNOWPACK model the role of the snow cover for the flood event. Confirming our model results, they concluded that the snow cover up to an elevation of 2000 m a.s.l. in the Loetschen valley was saturated when rain starts to fall. Singh et al. (1997) experimentally showed that saturated snow cover produces a very rapid runoff response and maximum melt flow. We conclude that the snow cover in the Loetschen valley was saturated before or shortly after the rain started to fall, depending on elevation. This enabled a rapid direct runoff during inten-

HESSD
10, 12861–12904, 2013

sive rainfall and explains the short response time in the Milibach tributary catchment where maximum precipitation occurred. Hence, the decrease of direct and interflow travel time in the hydrological model was found essential to reproduce the flood peak.

However, there are also some limitations in our findings: rapid snow melt release from snow cover is not reproduced in a physical manner in the hydrological model WaSiM-ETH, but rather captured by adjusting these runoff times. The adjustments of the runoff time are uncertain as they are not fitted against constantly measured discharge. WaSiM-ETH is further limited as it uses a fixed water holding capacity in the snow and homogenous snow structures. A coupling of WaSiM-ETH with a snow model might give a much better process representation.

Comparing our findings with the cited studies, our interpretation about the major processes and the model adjustments is confirmed. However, we were unable to simulate the estimated runoff-peak of 32 $m^3 s^{-1}$ in the Milibach catchment. This might be partly due to an underestimation of the measured rainfall, or it might be due to a further concentration of the runoff. In addition, because the flood peak was estimated by field observations, the estimated value itself is uncertain, even though it was performed by an expert (unpublished data, Geoplan Naturgefahren). Despite the extensive observations available in the Loetschen valley and even though we were able to reproduce the course of the event with a hydrological model, the exact flood magnitude in the Milibach catchment and the response time of the catchment remains uncertain due to uncertainties of observations and in the hydrological model.

Using the COSMO-2 forecast data as input to drive the optimized hydrological model, we found that the flood peak was substantially underestimated; the forecasted peak flow was a two year event (Lonza at Blatten gauge: 35 $m^3 s^{-1}$). We found a combination of insufficient precipitation and a weaker temperature increase than observed (during the night of 9 October to 10 October) that resulted in insufficient runoff. A reason for this underestimation might be an unrealistic representation of meteorological processes by COSMO-2 at a small scale like the Milibach catchment (3.3 km^2). The model performance of the COSMO-2 precipitation has been evaluated against coarser

HESSD
10, 12861–12904, 2013

resolution models and radar based observations by Weusthoff et al. (2010). They found that COSMO-2 to represent the convective precipitation such as the precipitation in the present study much better than coarser NWPs. Strikingly, the spatial pattern of the COSMO-2 precipitation (not shown here) was in good agreement with our station measurements. However, the temperature increase and precipitation amount were not well predicted. This underlines findings by Jasper et al. (2002) who emphasized the gross effect of small deviations in temperature and precipitation forecast data on hydrological projections.

5 Conclusions

The goal of this study was to reconstruct the hydro-meteorological anatomy of a rain-on-snow flood event, find the triggering processes, and estimate the predictability of the event. Firstly, we were able to trace the meteorological causes and the relevant hydrological process behind this event. Important atmospheric ingredients of the flood event were: (a) a combination of an atmospheric river that reached Switzerland after a cold period with significant snowfall, (b) potentially local rainfall enhancement by a cavity circulation, and (c) enhanced snow melt due to additional latent heat input from the warm and moist air. Overall, this study contributes to our understanding of other flood events that were triggered by an AR in Europe by adding another process region (Switzerland) and another process type (rain-on-snow event). Furthermore, we confirm previous studies on the importance of leeward circulation and latent and sensible heat fluxes during rain-on-snow flood events.

Secondly, considering this detailed knowledge on the meteorological input and locally enhanced precipitation pattern, we are able to reconstruct the flood peak, even at the subcatchment scale. The transfer of latent heat provided by precipitation and condensation, the rapid saturation of the snow cover and subsequent rapid runoff, and the activation of snow melt in a large part of the catchment were crucial processes. Exten-

Discussion Paper | Discussion Paper | Discussion Paper | Discussion Paper |

HESSD
10, 12861–12904, 2013

A non- forecasted rain-on- snow flood in the Alps

O. Rössler et al.

sive observations were necessary to provide enough information to adjust a standard hydrological model to this rain-on-snow flood.

Thirdly, despite the effort made to understand this flood event and to adjust the hydrological model, the ability of the hydro-meteorological model chain to predictive this rain-on-snow flood was limited, mainly because forecast errors were significant.

In addition, only with a dense network of "private" meteorological stations – despite all uncertainties due to unheated instruments – was it possible to reconstruct the local meteorological conditions that caused the flood. This stresses the need to maintain and extend the network of meteorological, snow and discharge gauging stations to improve and extent our observations and hence to improve future predictions. The good news is that while recent hydrological models need to be adjusted, they are capable of reacting sensitively to rain-on-snow events. Further studies on hydrological modeling of rain-on-snow events will be necessary to demonstrate the transferability of these adjustments to other events or regions.

The flood event on the 10th of October in the Loetschen valley was an enormous rain-on-snow event, caused by a temporally adverse sequence of otherwise typical or at least unproblematic processes. The flood can be reconstructed and predicted if the hydrological model is adjusted to react sensitively to these events and if the meteorological forecasts of precipitation and temperature are sufficiently accurate.

Acknowledgements. We would like to thank Jules Sailer from Geoplan Naturgefahren, Steg, for fruitful discussions and detailed information about the event. In addition, we acknowledge the kind provision of data by EnAlpin (gauge Ferden), MeteoMedia (meteorological station Wiler), SLF (meteorological and IMIS station Gandegg and Sackhorn), MeteoSwiss (official meteorological station data), BAFU (discharge from Lonza, Blatten), Urs Germann and Ioannis Sideris (MeteoSchweiz).

HESSD

10, 12861–12904, 2013

A non- forecasted rain-on- snow flood in the Alps

O. Rössler et al.

References

Anderson, E. A. (Ed.): National Weather Service River Forecast System: Snow Accumulation and Ablation Model, National Oceanographic and Atmospheric Administration (NOAA) Technical Memorandum NWS-HYDRO, 17, US Department of Commerce, Silver Spring, MD, 238 pp., 1973.

Andres, N., Badoux, A., Hilker, N., and Hegg, C.: Unwetterschäden in der Schweiz im Jahre 2011, Wasser, Energie, Luft, 104, 41–49, 2011.

Bao, J. W., Michelson, S., Neiman, P., Ralph, F. M., and Wilczak, J.: Interpretation of enhanced integrated water vapor bands associated with extratropical cyclones: their formation and connection to tropical moisture, Mon. Wea. Rev., 134, 1063–1080, doi:10.1175/MWR3123.1, 2006.

Barros, A. P. and Kuligowski, R. J.: Orographic effects during a severe wintertime rainstorm in the Appalachian Mountains, Mon. Wea. Rev., 126, 2648–2672, 1998.

Beven, K.: Rainfall-Runoff Modelling: the Primer, Wiley, Chichester, 2001.

Börst, U.: Nachhaltige Entwicklung im Hochgebirge: eine Systemanalyse von Mensch–Umwelt-Szenarien im Lötschental (Zentral-Alpen), Dissertation, Bonn, 214 pp., 2005.

Bundesamt für Umwelt (Ed.): Ereignisanalyse Hochwasser August 2007, Bern, 209 pp., 2009.

Cloke, H. and Pappenberger, F.: Ensemble flood forecasting: a review, J. Hydrol., 375, 613–626, doi:10.1016/j.jhydrol.2009.06.005, 2009.

Conway, H.: Storm Lewis: a rain-on-snow event on the Milford Road, New Zealand, in: International Snow Science Workshops (ISSW) Proceedings of Professional Papers and Poster Talks, 557–564, available at: http://arc.lib.montana.edu/snow-science/item.php?id=1137 (last access: 21 October 2013), 19–24 September 2004, Jackson Hole, Wyoming, 2004.

Dee, D. P., Uppala, S. M., Simmons, A. J., Berrisford, P., Poli, P., Kobayashi, S., Andrae, U., Balmaseda, M. A., Balsamo, G., Bauer, P., Bechtold, P., Beljaars, A. C. M., van de Berg, L., Bidlot, J., Bormann, N., Delsol, C., Dragani, R., Fuentes, M., Geer, A. J., Haimberger, L., Healy, S. B., Hersbach, H., Hólm, E. V., Isaksen, L., Kållberg, P., Köhler, M., Matricardi, M., McNally, A. P., Monge-Sanz, B. M., Morcrette, J.-J., Park, B.-K., Peubey, C., Rosnay, P. de, Tavolato, C., Thépaut, J.-N., and Vitart, F.: The ERA-Interim reanalysis: configuration and performance of the data assimilation system, Q. J. Roy. Meteor. Soc., 137, 553–597, doi:10.1002/qj.828, 2011.

HESSD

10, 12861–12904, 2013

A non- forecasted rain-on- snow flood in the Alps

O. Rössler et al.

Gray, W. R. and Seed, A. W.: The characterisation of orographic rainfall, Meteorol. Appl., 7, 105–119, 2000.
Green, W. and Ampt, G.: Studies of soil physics, part I – the flow of air and water through soils, J. Agr. Sci., 4, 1–24, 1911.
Houze, R. A. and Medina, S.: Turbulence as a mechanism for orographic precipitation enhancement, J. Atmos. Sci., 62, 3599–3623, 2005.
Jasper, K., Gurtz, J., and Lang, H.: Advanced flood forecasting in Alpine watersheds by coupling meteorological observations and forecasts with a distributed hydrological model, J. Hydrol., 267, 40–52, 2002.
Jones, E., Rango, A., and Howell, S.: Snowpack liquid water determinations using freezing calorimetry, Nord. Hydrol., 14, 113–126, 1983.
Kirchhofer, W. and Sevruk, B.: Mittlere jährliche korrigierte Niederschlagshöhen 1951–1980: Kartenblatt 2.2, in: Hydrologischer Atlas der Schweiz, BAFU, Bern, 2010.
Knippertz, P. and Wernli, H.: A lagrangian climatology of tropical moisture exports to the Northern Hemispheric extratropics, J. Climate, 23, 987–1003, doi:10.1175/2009JCLI3333.1, 2010.
Kroczynski, S.: A comparison of two rain-on-snow events and the subsequent hydrologic responses in three small river basins in Central Pennsylvania, Eastern Region Technical Attachment, 4, 1–21, 2004.
Lavers, D. A. and Villarini, G.: The nexus between atmospheric rivers and extreme precipitation across Europe, Geophys. Res. Lett., 40, 3259–3264, doi:10.1002/grl.50636, 2013.
Lavers, D. A., Allan, R. P., Wood, E. F., Villarini, G., Brayshaw, D. J., and Wade, A. J.: Winter floods in Britain are connected to atmospheric rivers, Geophys. Res. Lett., 38, L23803, doi:10.1029/2011GL049783, 2011.
Leathers, D. J., Kluck, D. R., and Kroczynski, S.: The severe flooding event of January 1996 across North-Central Pennsylvania, B. Am. Meteorol. Soc., 79, 785–797, 1998.
Marks, D., Kimball, J., Tingey, D., and Link, T.: The sensitivity of snowmelt processes to climate conditions and forest cover during rain-on-snow: a case study of the 1996 Pacific Northwest flood, Hydrol. Process., 12, 1569–1587, 1998.
McCabe, G. J., Hay, L. E., and Clark, M. P.: Rain-on-snow events in the Western United States, B. Am. Meteorol. Soc., 88, 319–328, doi:10.1175/BAMS-88-3-319, 2007.
Merz, R. and Blöschl, G.: A process typology of regional floods, Water Resour. Res., 39, 1340, doi:10.1029/2002WR001952, 2003.

MeteoSchweiz: Model Properties: Dynamics and Numerics, Physics, Data Assimilation, and more, available at: http://www.meteoschweiz.admin.ch/web/en/research/consortia/cosmo/ (last access: 16 August), 2013.
Ralph, F. M., Neiman, P. J., Wick, G. A., Gutman, S. I., Dettinger, M. D., Cayan, D. R., and White, A. B.: Flooding on California's Russian River: role of atmospheric rivers, Geophys. Res. Lett., 33, L13801, doi:10.1029/2006GL026689, 2006.
Reinecke, P. A. and Durran, D. R.: Estimating topographic blocking using a Froude number when the static stability is nonuniform, J. Atmos. Sci., 65, 1035–1048, doi:10.1175/2007JAS2100.1, 2008.
Roberts, N. M., Cole, S. J., Forbes, R. M., Moore, R. J., and Boswell, D.: Use of high-resolution NWP rainfall and river flow forecasts for advance warning of the Carlisle flood, north-west England, Met. Apps, 16, 23–34, doi:10.1002/met.94, 2009.
Rössler, O. and Löffler, J.: Potentials and limitations of modelling spatio-temporal patterns of soil moisture in a high mountain catchment using WaSiM-ETH, Hydrol. Process., 24, 2182–2196, doi:10.1002/hyp.7663, 2010.
Rössler, O., Diekkrüger, B., and Löffler, J.: Potential drought stress in a Swiss mountain catchment-Ensemble forecasting of high mountain soil moisture reveals a drastic decrease, despite major uncertainties, Water Resour. Res., 48, W04521, doi:10.1029/2011WR011188, 2012.
Rössler, O., Froidevaux, P., Börst, U., Rickli, R., Martius, O., and Weingartner, R.: Ereignisanalyse Extremhochwasser Lötschental, Wallis, 10. Oktober 2011, Publikation Gewässerkunde 553, GIUB, Bern, 2013.
Schlemmer, L., Martius, O., Sprenger, M., Schwierz, C., and Twitchett, A.: Disentangling the forcing mechanisms of a heavy precipitation event along the Alpine south side using potential vorticity inversion, Mon. Wea. Rev., 138, 2336–2353, doi:10.1175/2009MWR3202.1, 2010.
Schulla, J.: Model Description WaSiM, available at: http://www.wasim.ch/ (last access: 29 October 2013), 2013.
Singh, P., Spitzbart, G., Hübl, H., and Weinmeister, H.: Hydrological response of snowpack under rain-on-snow events: a field study, J. Hydrol., 202, 1–20, 1997.
Stohl, A., Forster, C., and Sodemann, H.: Remote sources of water vapor forming precipitation on the Norwegian west coast at 60° N – a tale of hurricanes and an atmospheric river, J. Geophys. Res., 113, D05102, doi:10.1029/2007JD009006, 2008.

HESSD
10, 12861–12904, 2013

A non- forecasted rain-on- snow flood in the Alps

O. Rössler et al.

Sui, J., Koehler, G.: Rain-on-snow induced flood events in southern Germany, J. Hydrol., 252, 205–220, 2001.
Verbunt, M., Gurtz, J., Jasper, K., Lang, H., Warmerdam, P., and Zappa, M.: The hydrological role of snow and glaciers in alpine river basins and their distributed modeling, J. Hydrol., 282, 36–55, doi:10.1016/S0022-1694(03)00251-8, 2003.
Whitaker, A. C. and Sugiyama, H.: Seasonal snowpack dynamics and runoff in a cool temperate forest: lysimeter experiment in Niigata, Japan, Hydrol. Process., 19, 4179–4200, 2005.
Weusthoff, T., Ament, F., Arpagaus, M., and Rotach, M. W.: Assessing the benefits of convection-permitting models by neighborhood verification: examples from MAP D-PHASE, Mon. Weather Rev., 138, 3418–3433, doi:10.1175/2010MWR3380.1, 2010.
Wirth, V., Kristen, M., Leschner, M., Reuder, J., and Schween, J. H.: Banner clouds observed at Mount Zugspitze, Atmos. Chem. Phys., 12, 3611–3625, doi:10.5194/acp-12-3611-2012, 2012.

HESSD
10, 12861–12904, 2013

Table 1. Meteorological stations in the catchment with the parameters measured, the elevation of the location, and the supporting institution.

ID (cp. Fig. 1)	Meteorological Station	Institution	Elevation, m a.s.l.	Temperature	Precipitation	Snow height	Wind speed	Wind direction	Relative humidity
1	Ried	GIUB	1470	×	×	×	×	×	×
2	Chumme	GIUB	2210	×	×	×	×	×	×
3	Grund	GIUB	1855	×	×	×	×	×	×
4	Grossi Tola	GIUB	2880	×	×	–	×	×	×
5	Mannlich	GIUB	2250	×	×	×	×	×	×
6	Sackhorn	SLF	3200	×	–	–	×	×	×
7	Gandegg	SLF	2717	×	×	×	×	×	×
8	Wiler	Meteomedia	1415	×	×	–	×	×	×

HESSD
10, 12861–12904, 2013

Table 2. Water fluxes, storages and characteristic values during the peak flow from 6 October to 10 October, 2011 for SM2 melt modules under standard and refined meteorology.

	Ferden (140 km^2)		Blatten (78 km^2)		Milibach (3.3 km^2)	
	Standard meteorology	refined meteorology	Standard meteorology	refined meteorology	Standard meteorology	refined meteorology
rain [mm]	93.6	94.5	75.5	77.4	92.6	167.9
snow [mm]	124.2	104.3	122.6	121.8	103.9	84.4
total runoff [mm]	102.2	95.7	92	80.3	109.3	188.4
direct flow [mm]	39.7	39.6	36.5	31.2	45.8	99.4
interflow [mm]	92.5	55.9	55.4	48.9	63.5	88.8
base flow [mm]	0	0.2	0	0.2	0	0.1
max. snow cover [mm]	85.3	62.3	102.9	79.6	97.3	72.1
snow cover after event [mm]	21.8	34.9	43.7	67.8	22.9	12.8
change in snow cover [mm]	−63.5	−27.4	−59.2	−11.8	−74.4	−59.3
Change in soil moisture [mm]	6.7	33.2	6.3	29.4	7.1	46.9
Rainfall–runoff-coefficient [1/1]	1.09	1	1.22	1	1.18	1.1
Snowmelt–runoff-ratio [1/1], Jasper et al. (2002)	0.62	0.3	0.64	0.1	0.68	0.3

HESSD
10, 12861–12904, 2013

A non- forecasted rain-on- snow flood in the Alps

O. Rössler et al.

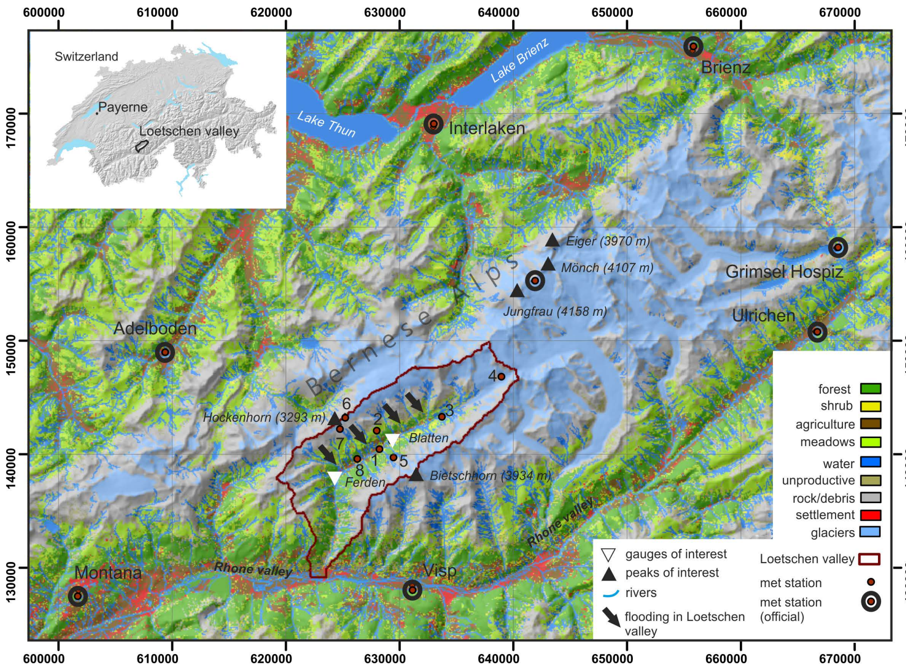

Fig. 1. Location of the Loetschen valley in Switzerland and the land cover characteristics of the valley. The black arrows indicate the flooding rivers, red dots and black circles represent meteorological stations, and white triangles represent discharge gauges.

HESSD
10, 12861–12904, 2013

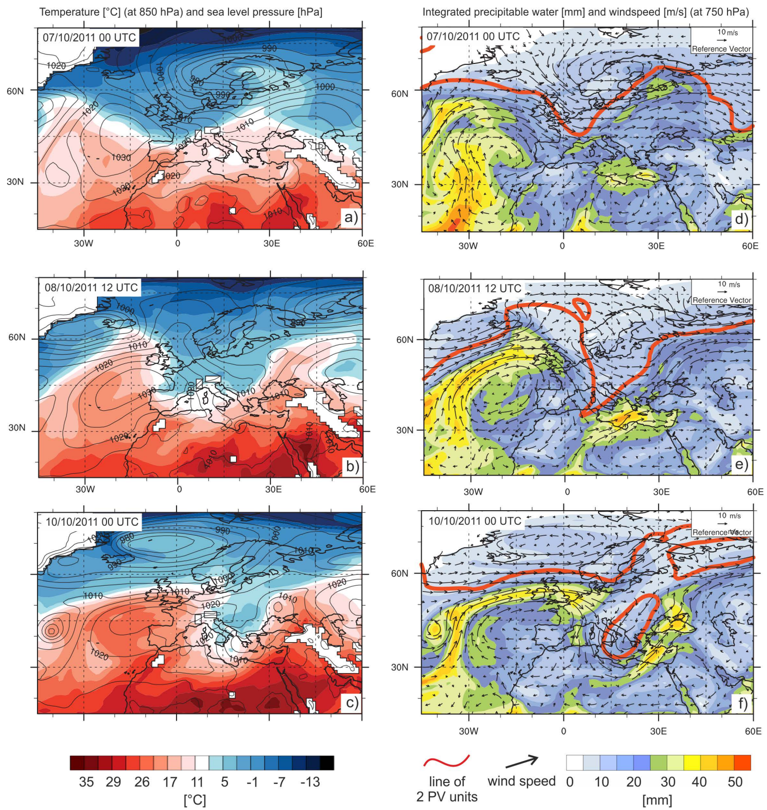

Fig. 2. ECMWF reanalysis data at 07 October 2011 00:00 UTC (top row), 08 October 2011 12:00 UTC (middle row) and 10 October 2011 00:00 UTC (bottom row). The left column displays temperature in K at 850 hPa (color) together with sea level pressure in hPa (contours) **(a–c)**. The right column shows the vertically integrated water content of the atmosphere in mm (color) together with the 850 hPa wind in m s^{-1} (arrows) **(d–f)**. The red line in these panels refers to the potential vorticity and illustrates the 2 PVU isoline on the 320 K isentrope.

HESSD
10, 12861–12904, 2013

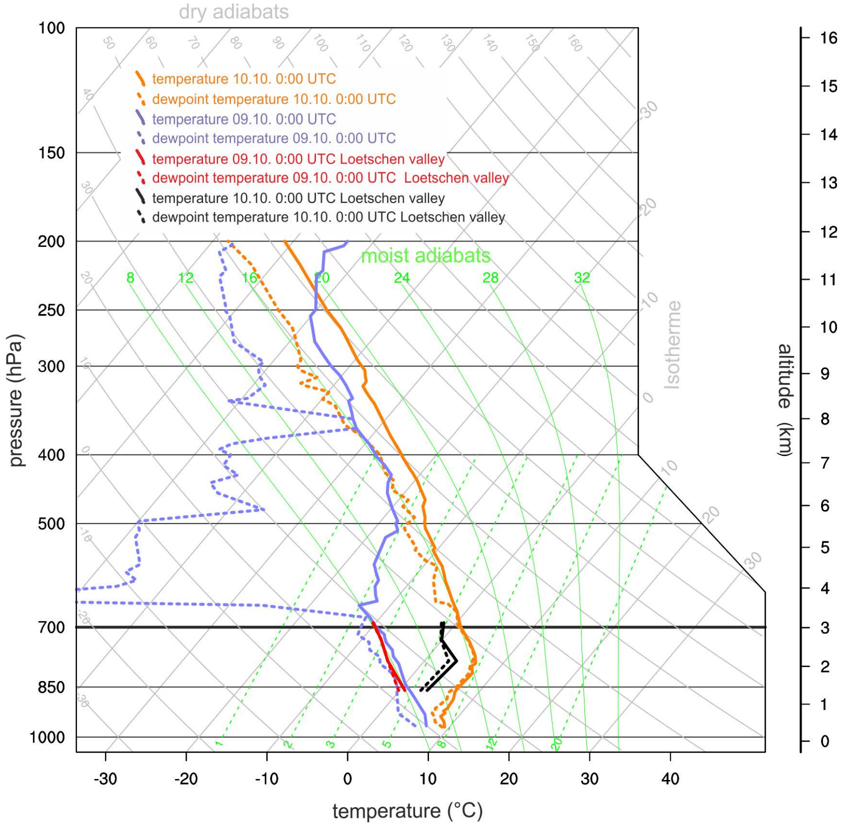

Fig. 3. Skew-*t*–log-*P*-diagram showing the vertical atmospheric structure as measured from weather balloons launched at Payerne (cf. Fig. 1) on 09 October 2011 00:00 UTC (blue lines) and 10 October 2011 00:00 UTC (orange lines). The profile of the Loetschen valley as retrieved by surface meteorological stations is included for comparison (red for 09 October 00:00 UTC and black for 10 October 00:00 UTC). The main ridge of the Loetschen valley has a mean elevation of approximately 3000 m a.s.l. (thick line).

HESSD
10, 12861–12904, 2013

A non- forecasted rain-on- snow flood in the Alps

O. Rössler et al.

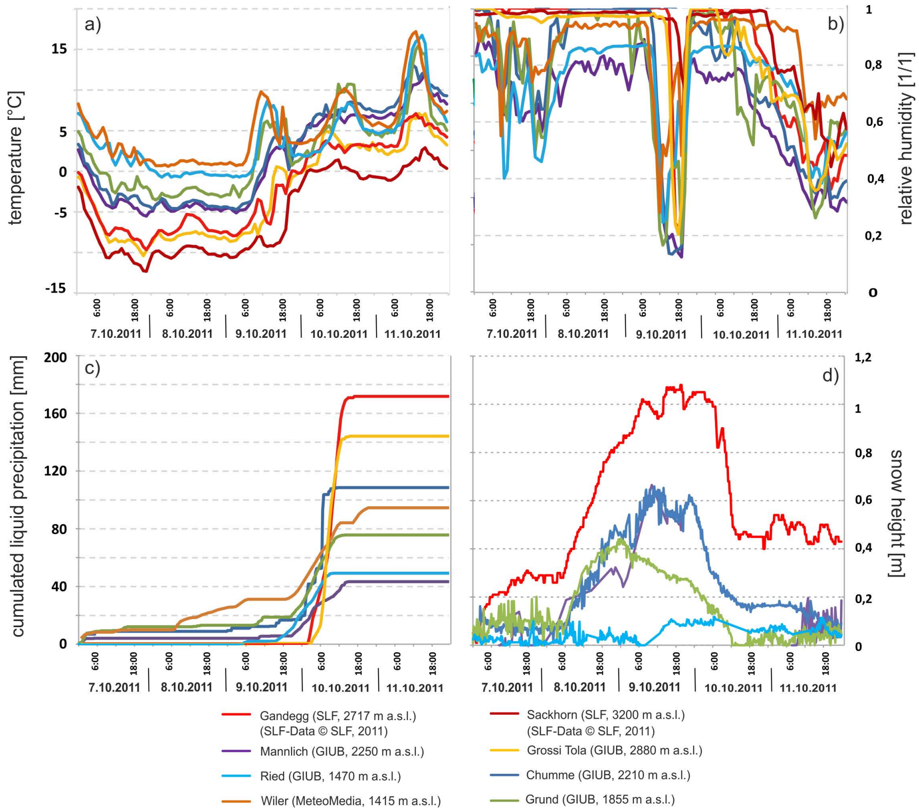

Fig. 4. Temperature **(a)**, relatively humidity **(b)**, accumulated liquid precipitation **(c)**, and snow height **(d)** measured at the eight meteorological stations in the Loetschen valley confirm the overall course of the weather and reveal a strong spatial concentration of rainfall.

HESSD
10, 12861–12904, 2013

A non- forecasted rain-on- snow flood in the Alps

O. Rössler et al.

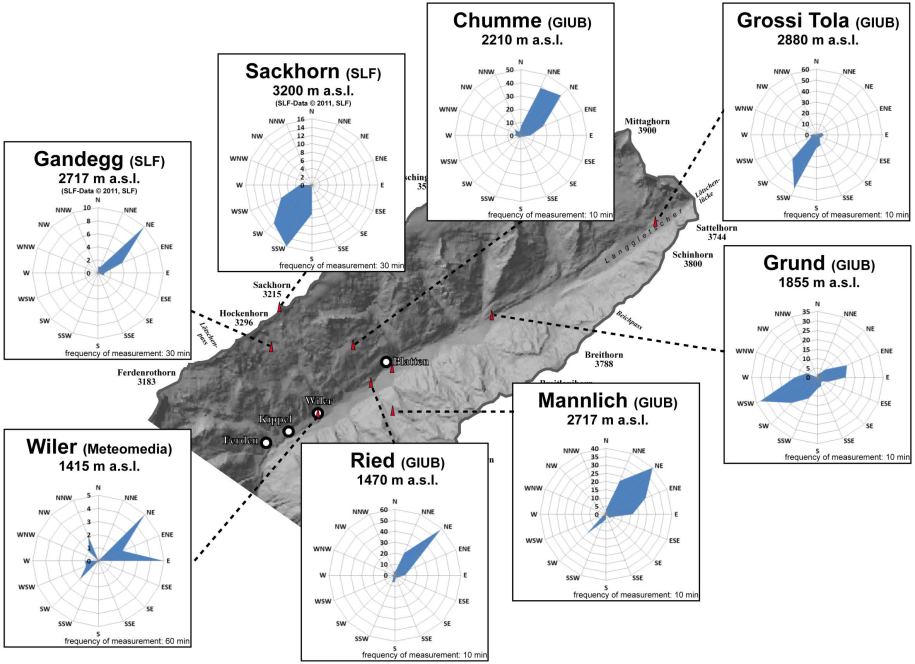

Fig. 5. Frequency of two-meter wind directions from station measurements on 10 October in the Loetschen valley. The radial component of each azimuth is proportional to its relative frequency.

HESSD
10, 12861–12904, 2013

A non- forecasted rain-on- snow flood in the Alps

O. Rössler et al.

Title Page
Abstract | Introduction
Conclusions | References
Tables | Figures
◀| |▶
◀ ▶
Back | Close
Full Screen / Esc
Printer-friendly Version
Interactive Discussion

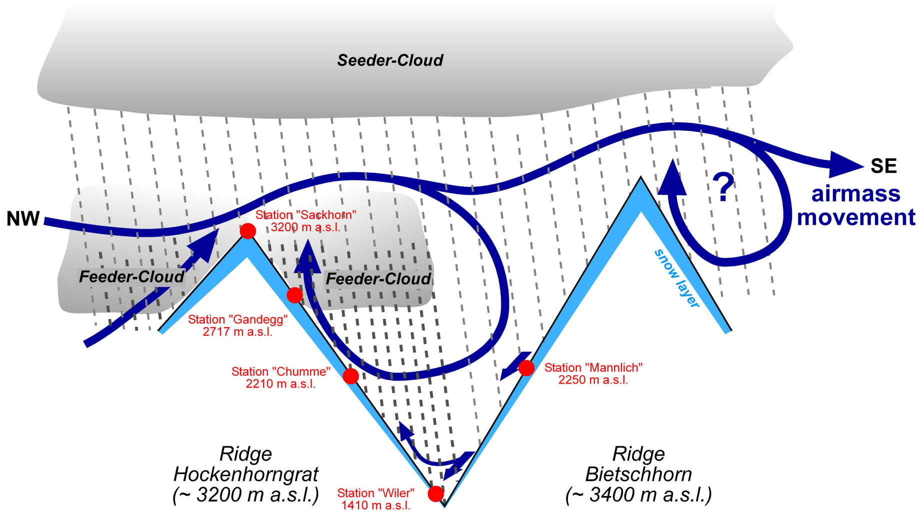

Fig. 6. Schematic depiction of our interpretation of the atmospheric conditions.

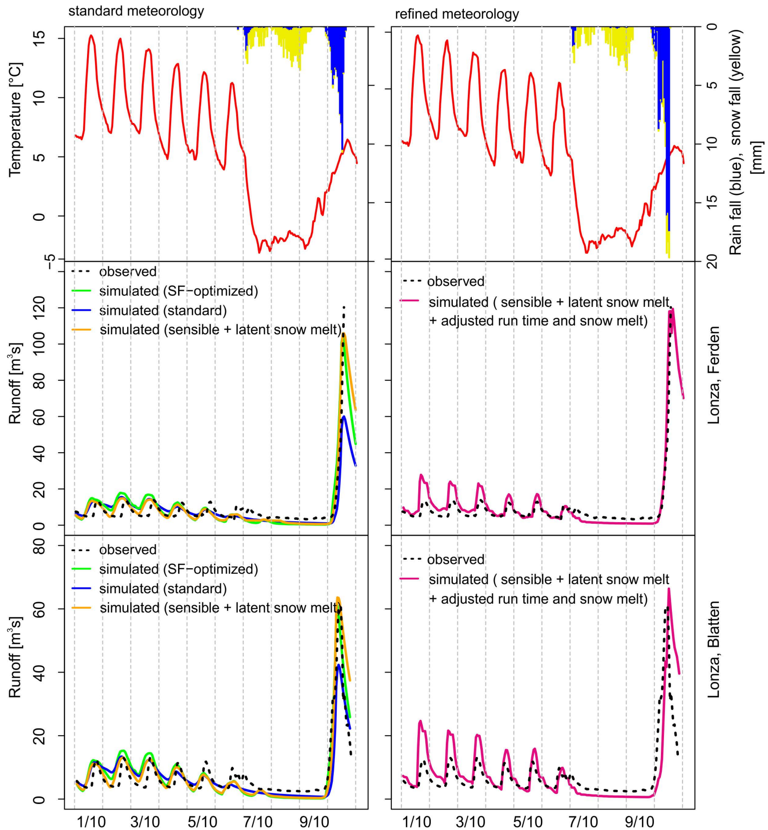

Fig. 7. Retrospective modeling of the flood event at two gauges, Lonza, Ferden and Lonza, Blatten, under standard (left panel) and refined meteorology (right panel) shows that the standard WaSiM-ETH model set up (blue line) is not able to replicate the observations (black lines), while the three peak-optimized model set ups are capable of matching the observations (orange, green, magenta lines). Meteorological is depicted as temperature (red line) and rainfall (blue) and snowfall (yellow) in the top row.

HESSD
10, 12861–12904, 2013

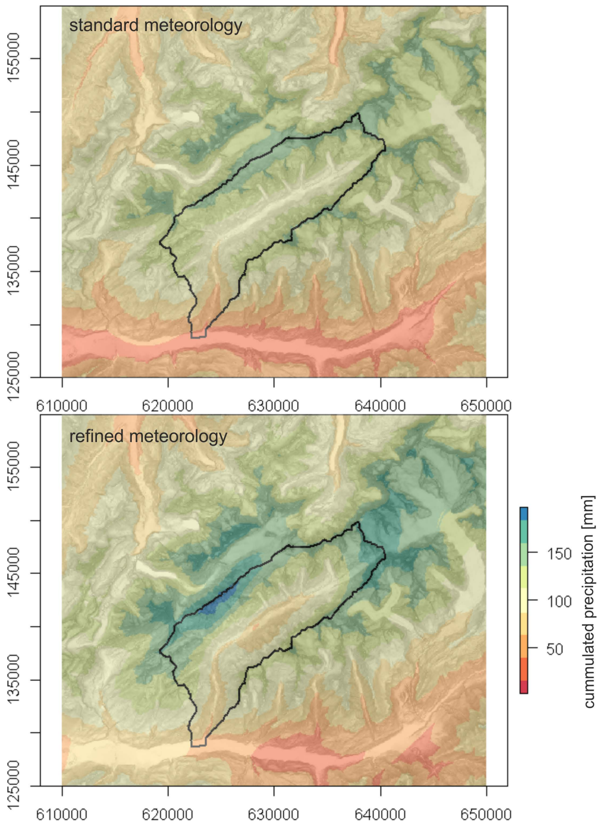

Fig. 8. Accumulated liquid precipitation from 9 October 14:00 UTC to 10 October 20:00 UTC, as regionalized by the hydrological model using to the inverse distant and height regression approaches with the official meteorological stations and the SLF Gandegg station (cp. Fig. 1), upper panel, and using the refined meteorology with all available meteorological stations with a correction function (lower panel) and a fixed southwest-northeast interpolation orientation following the topography.

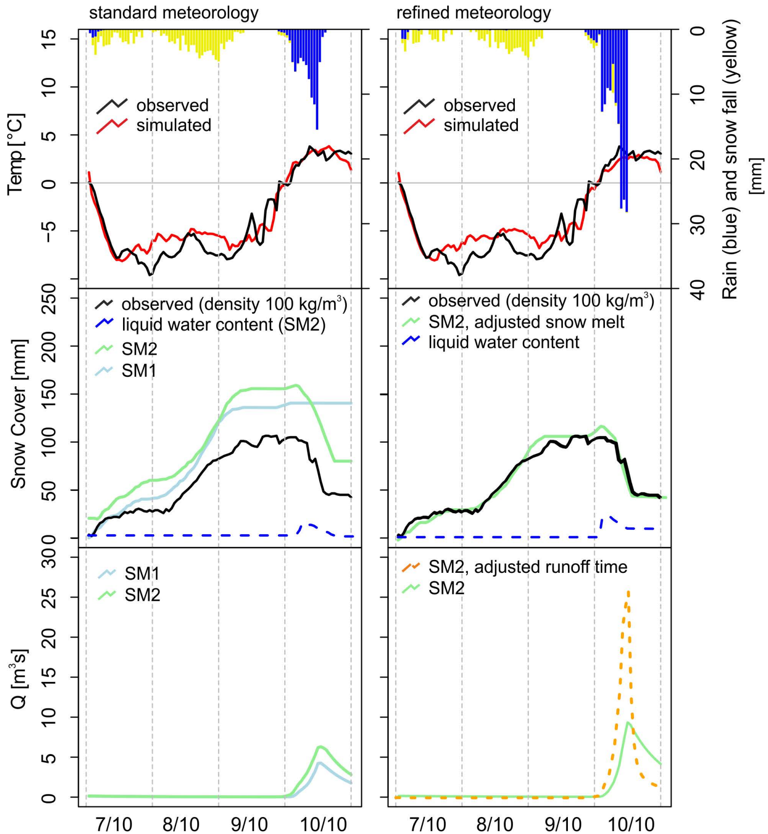

Fig. 9. Model performances with standard and refined meteorology for precipitation and temperature (top row), snow depth (center row) and runoff (lower row) for the tributary river Milibach. Dashed blue line depicts the liquid water content in the snow cover. Refined meteorology and snow melt from latent and sensible heat are able to reproduce both snow cover accumulation and depletion.

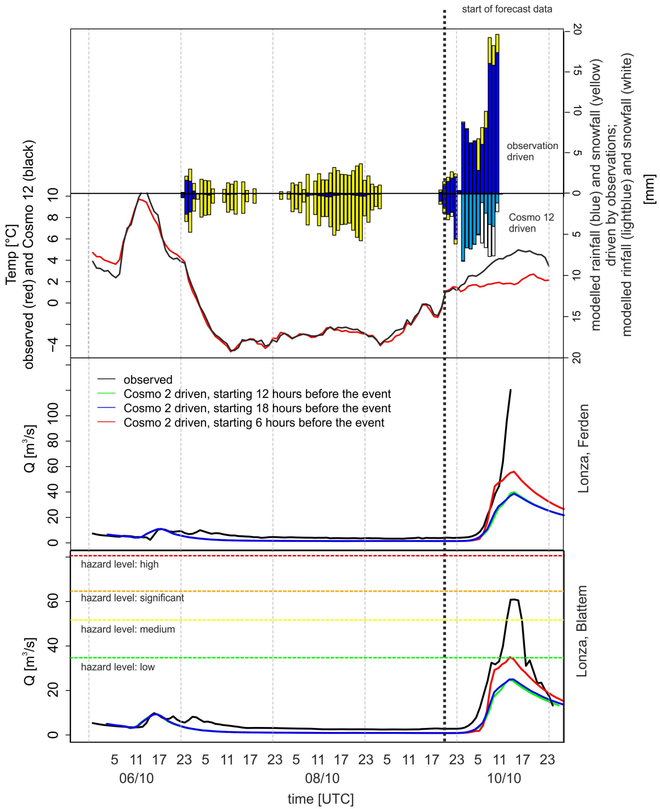

Fig. 10. Simulated discharge at Lonza, Ferden and Lonza, Blatten using the best adjusted hydrological model with COSMO-2 data 6, 12, and 18 h in advance. The temperature and the solid and liquid precipitation are average values for the entire valley taken from COSMO-2, 12 h in advance. The blue and yellow bars and black line indicate observed rain, snow, and temperature of the refined meteorology, respectively. Hazard levels are official hazard levels corresponding to a 2 yr, 10 yr, 30 yr, and 100 yr event.